High Temperature Magnetic Stabilization of Cobalt Nanoparticles by an Antiferromagnetic Proximity Effect

José A. De Toro,[1,*] Daniel P. Marques,[1] Pablo Muñiz,[1] Vassil Skumryev,[2,3] Jordi Sort,[2,3] Dominique Givord,[4,5,6,†] and Josep Nogués[3,7,‡]

[1]*Instituto Regional de Investigación Científica Aplicada (IRICA) and Departamento de Física Aplicada, Universidad de Castilla-La Mancha, E-13071 Ciudad Real, Spain*
[2]*Departament de Física, Universitat Autònoma de Barcelona, E-08193 Bellaterra, Barcelona, Spain*
[3]*Institució Catalana de Recerca i Estudis Avançats (ICREA), Barcelona, Spain*
[4]*Université Grenoble Alpes, Institut NEEL, F-38042 Grenoble, France*
[5]*CNRS, Institut NEEL, F-38042 Grenoble, France*
[6]*Instituto de Fisica, Universidade Federal do Rio de Janeiro, Rio de Janeiro, Rio de Janeiro, 21941-972, Brasil*
[7]*ICN2–Institut Catala de Nanociencia i Nanotecnologia, Campus UAB, E-08193 Bellaterra, Barcelona, Spain*

(Received 3 February 2015; revised manuscript received 1 May 2015; published 28 July 2015)

Thermal activation tends to destroy the magnetic stability of small magnetic nanoparticles, with crucial implications for ultrahigh density recording among other applications. Here we demonstrate that low-blocking-temperature ferromagnetic (FM) Co nanoparticles ($T_B < 70$ K) become magnetically stable above 400 K when embedded in a high-Néel-temperature antiferromagnetic (AFM) NiO matrix. The origin of this remarkable T_B enhancement is due to a magnetic proximity effect between a thin CoO shell (with low Néel temperature, T_N, and high anisotropy, K_{AFM}) surrounding the Co nanoparticles and the NiO matrix (with high T_N but low K_{AFM}). This proximity effect yields an effective antiferromagnet with an apparent T_N beyond that of bulk CoO, and an enhanced anisotropy compared to NiO. In turn, the Co core FM moment is stabilized against thermal fluctuations via core-shell exchange-bias coupling, leading to the observed T_B increase. Mean-field calculations provide a semiquantitative understanding of this magnetic-proximity stabilization mechanism.

DOI: 10.1103/PhysRevLett.115.057201 PACS numbers: 75.75.-c, 75.30.Et, 75.50.Ee

The current miniaturization trend in magnetic applications has led to a quest to suppress spontaneous thermal fluctuations (superparamagnetism) in ever-smaller nanostructures [1–5]; this is a clear example of the fundamental efforts of condensed matter physics to meet technological challenges [6] (e.g., the continued growth of recording density [7]). Despite the foreseeable change of the recording paradigm from continuous to patterned media, where each bit is recorded in an individual nanostructure [7], the key for sustained storage density increase will remain the introduction of progressively more anisotropic (high-K) materials [8], which allow for magnetic stability at very small volumes, V [i.e., blocking temperature, $T_B \propto KV$, above room temperature (RT)]. Two main strategies are primarily investigated to achieve high K, both of them with implications in other active technologies beyond information storage, such as permanent magnets, magnetic hyperthermia, or even sensors [5,9–11]. These are (i) the use of compounds with intrinsically high magnetocrystalline anisotropy (such as FePt [3,8]) and (ii) the design of exchange-coupled nanocomposites [4,12–29]. Unfortunately, most high-K materials require high-temperature annealing processes to obtain the desired phase, which could hamper their implementation in certain structures. Thus, ferromagnetic-antiferromagnetic (FM-AFM) exchange coupling alternatives may be an appealing option. In fact, it has been demonstrated [4] that FM-AFM interfacial exchange coupling is an effective method (later patented by Seagate [12]) to increase the effective K of FM nanoparticles. However, a T_B enhancement beyond RT using this approach has been rarely reported [22–26], and often broad particle-size distribution can partly account for the "apparent" T_B increase [22–25]. The reason for this scarcity is that high-Néel-temperature (T_N) AFMs tend to have a low anisotropy constant (e.g., NiO), and vice versa (e.g., CoO), while substantial values of *both* properties are required for high-temperature stabilization. This limitation could, in principle, be overcome by exploiting proximity effects, i.e., the interfacial synergetic hybridization of the properties of two AFM materials having complementary properties (here, high T_N and high K). Although this phenomenon is best known in superconductivity [30], proximity effects in bi- or multilayered magnetic systems (i.e., *magnetic* proximity effects) have also been studied [31]. In contrast, and despite their strong technological presence, proximity effects involving nanoparticles have hardly been explored [32,33].

In this Letter we demonstrate a proximity effect between two AFMs (a CoO shell and a NiO matrix) on FM particles (Co) and the resulting thermal stabilization of the NPs well

above RT (with a ~ tenfold enhancement of T_B to exceed 400 K), and we propose a mean-field model to gain insight into the nature of such an AFM proximity effect.

Three films of Co/CoO core or shell nanoparticles [4,34–36] (5–7 nm) highly dispersed in an AFM NiO matrix (S series)—see Fig. 1(a)—or in a Nb matrix, for reference (R series), were grown by combining inert gas condensation (Co nanoparticles) and rf sputtering (NiO and Nb) [34–40]. The digits in the sample names refer to the cluster source power (W), which, together with the occasional use of a carrier gas (He), was varied to control the nanoparticle size [35].

The low-temperature hysteresis loops of the Co/CoO-NiO samples (S series) measured after field cooling are shown in Fig. 1(b). The loops show rather large coercivities ($\mu_0 H_C \sim 0.4$ T) and loop shifts (i.e., H_E, the exchange bias field) $\mu_0 H_E \sim 0.4$ T. In contrast, the loops exhibit a rather small vertical shift (less than 1% of M_S). In the reference samples, where NiO is replaced by Nb (R series), H_C is considerably smaller ($\mu_0 H_C \sim 10$ mT) and no loop shifts are observed [Fig. 1(b), inset].

Remarkably, the $T = 300$ K hysteresis loops shown in Fig. 1(c) provide evidence that the samples are not superparamagnetic (i.e., with remanence M_R and $H_C > 0$). Not only is $\mu_0 H_C \sim 6$ mT, but H_E is surprisingly large (e.g., $\mu_0 H_E = 14$ mT for S50He). In contrast, the reference samples have vanishing M_R and H_C at $T = 300$ K, revealing their superparamagnetic state (Fig. S1 [34]). To assess the effect of coupling on the value of the superparamagnetic T_B, the field-cooled (FC) and zero-field-cooled (ZFC) temperature dependence of the magnetization, $M(T)$, was measured for two Co/CoO-NiO and Co/CoO-Nb films (S80 and R80, the largest particles, and S50He and R50He, the smallest particles) [Figs. 2(a) and 2(b)]. The $M(T)$ curves of the reference samples show the typical behavior of nanometric Co nanoparticles: T_B (taken as the maximum of the ZFC curve) is low and increases with particle size [i.e., $T_B(R50\text{He}) \approx 35$ K and

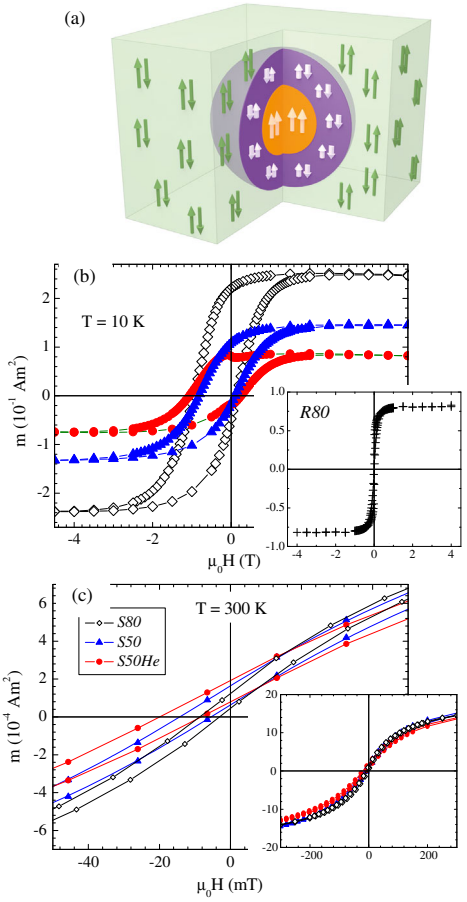

FIG. 1 (color online). (a) Schematic representation of the Co/CoO-NiO sample. (b) Field-cooled hysteresis loops of the Co/CoO-NiO samples (S series) at 10 K. Shown in the inset is the 10-K hysteresis loop of R80. (c) Field-cooled hysteresis loops of the same samples at 300 K. Shown in the inset are the same loops up to higher fields.

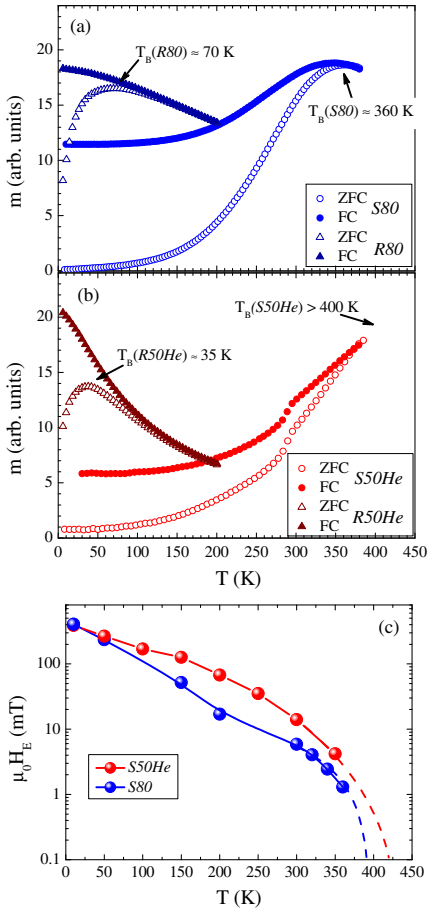

FIG. 2 (color online). FC or ZFC magnetization curves measured in 20 mT for (a) S80 and R80 and (b) S50He and R50He. The T_B values of the four samples are highlighted by arrows. (c) Temperature dependence of H_E for S80 and S50He. The continous lines are guides to the eye. The dashed curves are tentative extrapolations of $H_E(T)$ to hint $T_B[H_E]$.

$T_B(R80) \approx 70$ K]. In contrast, T_B for the Co/CoO-NiO samples is beyond RT [$T_B(S80) \approx 360$ K], and is even above 400 K (the maximum experimentally attainable temperature) for the case of $S50$He. The temperature dependence of H_E [Fig. 2(c)], which establishes the exchange-bias blocking temperature, $T_B[H_E]$, shows a similar trend to the superparamagnetic T_B, with H_E remaining finite probably above $T = 400$ K.

The present results demonstrate that Co nanoparticles of a few nm can be made magnetically stable above RT, up to at least $T = 400$ K [41]. The origin of the enhanced magnetic stability must reside in some coupling existing between the Co nanoparticles and the high-T_N AFM matrix, NiO ($T_N = 520$ K), since using CoO alone as the matrix limits the T_B enhancement to 290 K [T_N(CoO)] [4]. However, NiO is known to have a low anisotropy [42], leading to small H_E and low $T_B[H_E]$ (often below RT) [25,27,43–46]. This highlights that using a high-T_N material is not sufficient in itself to reach high-temperature stability.

The first indication of the origin of the observed effects is the very large H_E measured in the Co/CoO-NiO series at $T = 10$ K. NiO alone cannot induce such high H_E values; hence, the highly anisotropic CoO shell must be involved in the H_E enhancement. However, isolated Co/CoO nanoparticles with a thin (naturally oxidized) CoO shell usually exhibit very small H_E [39,40]. Three main types of processes have been proposed to achieve large H_E in Co/CoO systems [4,13–15,47]: (i) forced oxidation of the Co particles to form thick AFM CoO shells [13–15], (ii) matching the crystallographic structure between the CoO shell and the matrix (which structurally stabilizes the CoO shell) [47], and (iii) coupling the CoO shell to an AFM matrix (magnetic stabilization) [4]. Our low-oxygen synthesis method allows us to safely rule out the first possibility [13,15]. Because the crystalline structures of NiO and CoO are similar, both structural and magnetic stabilizations of the CoO shell are *a priori* plausible. However, the high values (above 400 K) of the superparamagnetic T_B and $T_B[H_E]$ imply that the magnetic stabilization cannot be solely a structural effect. Indeed, NiO may structurally stabilize CoO; nevertheless, the T_N of CoO ($T_N = 290$ K) is too low to cause the observed high-temperature effects. Consequently, the outstanding enhancement of the T_B of the Co nanoparticles must be a combined magnetic effect involving both the CoO shell and the NiO matrix.

In thin film systems it has been previously observed that H_E and $T_B[H_E]$ of NiFe/NiO bilayers can be tailored by inserting a thin CoO layer at the interface between both layers, i.e., NiFe/CoO/NiO [48,49]. When the CoO interfacial layer remains below 3 nm, $T_B[H_E]$ persists above $T = 400$ K, whereas for thicker CoO, it drops quickly to T_N(CoO). This effect can be understood as a *magnetic proximity effect* [31], where the overall properties of AFM_1/AFM_2 systems are the combination of both counterparts [50–52]. This concept has been recently applied to other types of AFMs such as IrMn/FeMn [53], and it must take place in the Co/CoO-NiO system, where the overall T_B is determined by the combined effect of the CoO shell coupled to the NiO matrix. However, to explain the high-temperature stability of the Co nanoparticles, a polarization of the Co AFM moments in the CoO shell is not sufficient; the overall anisotropy of the CoO-NiO couple, ultimately felt by the Co particles, must also remain sufficiently high. Consequently, the proximity effect between CoO and NiO has a twofold consequence, in which both the Co-induced magnetization and the overall anisotropy are involved [54].

For systems composed of FM nanoparticles embedded in an AFM matrix, H_E is classically expressed as

$$\mu_0 H_E M_{\mathrm{FM}} V = \gamma A \tag{1}$$

where M_{FM} is the FM magnetization, V is the volume of the ferromagnet, γ is the interfacial coupling energy per unit surface area, and A is the associated surface area. The evaluation of γ_0, the 0 K coupling energy, constitutes the major difficulty in the analysis of exchange-bias systems. Here, γ_0 is only taken as an experimental parameter. Naively, the temperature dependence of γ should be proportional to the interfacial AFM staggered magnetization (neglecting the temperature dependence of the FM Co nanoparticle magnetization). Given the complexity of experimentally obtaining the surface magnetization of the CoO nanoparticles, we have developed a simple molecular field model [34]. The mean field was determined by considering exchange interactions between nearest neighbors, in agreement with the short-range nature of superexchange interactions. An excellent agreement was obtained between the calculated temperature dependence of the CoO bulk staggered magnetization, assuming $S = 3/2$, and previous experimental results [55] [Fig. S2(a) [34]]. The temperature dependence of the surface magnetization was then calculated by assuming that, for surface atoms, the number of neighbors is reduced from 12 in the bulk to 9. The temperature dependence of the surface magnetization [Fig. S2(b) [34]] is reminiscent of the temperature dependence of the remanent magnetization in CoO nanoparticles, which has been related to surface magnetic moments [55]. Additionally, the calculated variation of the surface magnetization reproduces correctly the temperature dependence of H_E in the Co/CoO-CoO system (i.e., Co/CoO nanoparticles embedded in a CoO matrix [4]) in the whole temperature range—compare the calculated temperature dependence of the CoO surface magnetization in Fig. S2 [34] to the experimental $\mu_0 H_E(T)$ in Fig. S3 [34].

Obviously, expression (1) cannot explain the sizable H_E measured in the Co/CoO-NiO system at temperatures above the T_N of CoO, if the CoO shell has the same

properties as in Co/CoO [Fig. 2(c)]. Considering that the T_N of NiO (520 K) is much higher than that of CoO, it is natural to attribute the persistence of exchange-bias effects to a polarization of the Co moments by the Ni ones. To describe such a magnetic proximity effect, the molecular field model is applied to a stack of atomic shells covering a Co sphere of diameter 5 nm. The five most external shells are assumed to be made of pure NiO; they are followed by three intermixed shells where the fraction of Ni atoms decreases from 0.75 to 0.5 and 0.25, and by two shells of pure CoO. The assumed CoO/NiO interlayer mixing is consistent with reported observations in CoO/NiO multilayers prepared by sputtering [52]. Moreover, the total pure CoO equivalent thickness (≈1 nm corresponding to two pure CoO layers, each 0.268 nm thick, plus 1.5 equivalent CoO layers from the three intermixed layers) is consistent with the oxygen-poor synthesis conditions of the nanoparticles. In the model, a given atom has 12 neighbors in total: six neighbors in the shell it belongs to, and $3\alpha_p$ (α_m) atoms in the preceding (next) shells, where the coefficients α_p (α_m) are proportional to the respective surface area of each considered shell [34]. Calculations then reveal that a significant magnetization is maintained in CoO above its bulk T_N [red line in Fig. S2(b) [34]] via the proximity effect with NiO. Since the Co atoms in CoO at the interface with the core are directly exchange-coupled to the Co FM core (and, consequently, directly involved in exchange bias), the existence of a significant CoO-staggered magnetization above T_N(CoO) directly accounts for the persistence of exchange bias in this temperature range. Note that due to the short-range nature of the interactions, the NiO-induced polarization of CoO at the CoO/Co interface becomes negligible if more than two nonintermixed CoO layers are considered.

Although this calculation demonstrates that proximity effects in Co/CoO-NiO can account for H_E above T_N(CoO), it does not explain the rapid decrease of H_E with increasing temperature in Co/CoO-NiO compared to Co/CoO-CoO (compare Fig. 3 and Fig. S3 [34]). Actually,

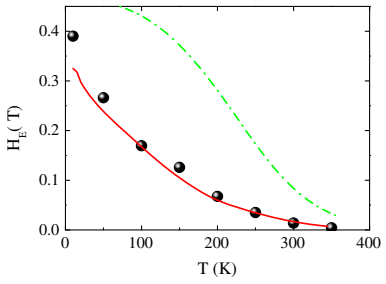

FIG. 3 (color online). Temperature dependence of H_E for Co/CoO-NiO: Experimental data for sample *S*50He (filled circles); calculated temperature dependence of H_E, neglecting thermal activation (dashed dotted lines); and taking thermal activation into account (solid line).

the AFM component in exchange-biased systems is usually composed of nanosized grains, which are prone to superparamagnetic effects [56]. To account for the possible existence of superparamagnetic CoO grains, a reduction coefficient must be applied to H_E in Eq. (1),

$$H_E = H_E^0 f^{2/3}, \tag{2}$$

where the parameter f represents the volume fraction of AFM grains involved in FM-AFM coupling and H_E^0 represents H_E-neglecting thermal activation effects. The 2/3 power accounts for the interfacial nature of the FM-AFM coupling. The condition for superparamagnetism is taken as $\Delta E < 25\ k_B T$, where ΔE is the energy barrier and k_B is the Boltzmann constant. The main term in ΔE is the anisotropy energy $K_{\mathrm{AFM}} V_{\mathrm{AFM}}$, where K_{AFM} and V_{AFM} are the anisotropy and volume of the AFM grains. The AFM grains are assumed to be composed of a CoO-NiO mixture, the minor CoO fraction being at the interface with the FM nanoparticle. The NiO magnetocrystalline anisotropy is considered negligible [42]; thus $K_{\mathrm{AFM}} V_{\mathrm{AFM}} \approx K_{\mathrm{CoO}} V_{\mathrm{CoO}}$, where K_{CoO} is the CoO magnetocrystalline anisotropy and V_{CoO} is the volume of the CoO part in each of the oxide grains forming the shell [34]. A Gaussian distribution of energy barriers is assumed. The best fit to the experimental data was obtained for $K_{\mathrm{CoO}} V_{\mathrm{CoO}} = 0.5 \times 10^{-20}$ J, with a standard deviation $\sigma = 0.25 \times 10^{-20}$ J, at 0 K. Assuming the bulk CoO magnetocrystalline anisotropy value at low temperatures, $K_{\mathrm{CoO}} = 0.4 \times 10^7$ J/m^3 [42], yields $V_{\mathrm{CoO}} = 1.25$ nm^3; this, in turn, corresponds to a CoO layer approximately 0.25 nm thick for cylindrical nanograins 2.5 nm in diameter [34]. This value compares reasonably with the 1-nm CoO equivalent thickness assumed in the calculation of proximity effects, given the uncertainty in the number of AFM grains forming the shell and the reduced magnetocrystalline anisotropy typically found in CoO thin shells due to reduced crystallinity [39,40] (which would actually imply thicker CoO grains). The temperature dependence of the anisotropy of the AFM, K_{AFM}, is assumed to be proportional to the cube of the reduced staggered magnetization as expected for second-order anisotropy. The experimental $H_E(T)$ data are semiquantitatively reproduced (Fig. 3) assuming Co nanoparticles 5 nm in diameter, in agreement with TEM observations (Fig. S4), and $\gamma_0 = 1.1 \times 10^{-3}$ J/m^2, consistent with literature data for Co/CoO [57]. The success of the model demonstrates that the rapid decrease of H_E with increasing temperature is linked to the moderate average anisotropy energy of the effective (mixed CoO-NiO) AFM grains, exchange-coupled to the Co nanoparticles. Thermal activation effects in such AFM grains (yielding a distribution of $T_B[H_E]$) are also evidenced by the shape of the ZFC $M(T)$ curves (Fig. 2), where the magnetization increases smoothly from low temperatures, in contrast with the relatively abrupt

increase (unblocking) observed in exchange-biased systems where a *single* $T_B[H_E]$ value is expected [58,59].

As a consistency test of our model, the temperature dependence of H_E in the Co/CoO-CoO system was recalculated using the same parameters as above (red line in Fig. S3 [34]). As in Co/CoO-NiO, the calculated curves (with the interfacial coupling coefficient γ_0 as an adjustable parameter) give a fair account of the experimental data. The theoretical curves obtained with $\gamma_0 = 1.3 \times 10^{-3}$ J/m^2, respectively accounting for and neglecting thermal activation, differ only slightly close to T_N (Fig. S3 [34]); this indicates that in the Co/CoO-CoO system, only a minor fraction of the AFM grains become superparamagnetic as temperature is increased. This situation is related to the high K_{AFM} characteristic of CoO [42]. All together, these results reflect the dual role of CoO and NiO in the magnetic stabilization of Co nanoparticles; i.e., while NiO contributes with high T_N, CoO supplies the high anisotropy.

In conclusion, we have presented the foremost example of exchange-bias particle stabilization exploiting magnetic proximity effects. Co/CoO core or shell (~5–7 nm) nanoparticles with blocking temperatures below 70 K have been stabilized well beyond 400 K by combining high-anisotropy CoO and high-T_N NiO antiferromagnets in a shell-matrix configuration; this provides an AFM anisotropy at the interface strong enough to enhance the effective anisotropy of the Co cores. A mean-field model, corrected for thermal activation effects, closely reproduces the experimental exchange-bias data, corroborating the above interpretation and illustrating the nature of the proposed proximity effect. The results presented in this Letter constitute a striking illustration of how a subtle combination of interactions may permit the occurrence of unique magnetic properties by exploiting proximity effects in magnetism. A similar approach could be applied to other composite systems, in and beyond magnetism, where proximity effects may be engineered to enhance the functionality of materials [30,60–64].

J. A. D. T. thanks P. S. Normile and R. López Antón for useful discussions and J. A. González and J. P. Andrés for technical advice. This work has been supported by projects from the Junta de Comunidades de Castilla-La Mancha [Grant No. PEII11-0226-8769] and from the Generalitat de Catalunya (Grant No. 2014-SGR-1015). D. P. Marques acknowledges support from the Brazilian CNPQ. ICN2 acknowledges support from the Severo Ochoa Program (MINECO, Grant No. SEV-2013-0295).

*JoseAngel.Toro@uclm.es
†Dominique.Givord@neel.cnrs.fr
‡Josep.Nogues@uab.cat

[1] D. Weller and A. Moser, IEEE Trans. Magn. **35**, 4423 (1999).
[2] M. Knobel, W. C. Nunes, L. M. Socolovsky, E. De Biasi, J. M. Vargas, and J. C. Denardin, J. Nanosci. Nanotechnol. **8**, 2836 (2008).
[3] J. P. Wang, Proc. IEEE **96**, 1847 (2008).
[4] V. Skumryev, S. Stoyanov, Y. Zhang, G. Hadjipanayis, D. Givord, and J. Nogués, Nature (London) **423**, 850 (2003).
[5] A. López-Ortega, M. Estarder, G. Salazar-Alvarez, A. G. Roca, and J. Nogués, Phys. Rep. **553**, 1 (2015).
[6] Physics gets its hands dirty, Editorial, Nat. Mater. **14**, 361 (2015).
[7] B. D. Terris and T. Thomson, J. Phys. D **38**, R199 (2005).
[8] G. W. Qin, Y. P. Ren, N. Xiao, B. Yang, L. Zuo, and K. Oikawa, Int. Mater. Rev. **54**, 157 (2009).
[9] F. Liu, J. Zhu, W. Yang, Y. Dong, Y. Hou, C. Zhang, H. Yin, and S. Sun, Angew. Chem., Int. Ed. **53**, 2176 (2014).
[10] S. H. Noh, W. Na, J. T. Jang, J. H. Lee, E. J. Lee, S. H. Moon, Y. Lim, J. S. Shin, and J. Cheon, Nano Lett. **12**, 3716 (2012).
[11] A. Weddemann, I. Ennen, A. Regtmeier, C. Albon, A. Wolff, K. Eckstädt, N. Mill, M. K. H. Peter, J. Mattay, C. Plattner, N. Sewald, and A. Hütten, Beilstein J. Nanotechnol. **1**, 75 (2010).
[12] B. Liu and D. K. Weller, U.S. Patent No. 71 58 346 (2007).
[13] J. B. Tracy, D. N. Weiss, D. P. Dinega, and M. G. Bawendi, Phys. Rev. B **72**, 064404 (2005).
[14] J. M. Riveiro, J. A. De Toro, J. P. Andrés, J. A. González, T. Muñoz, and J. P. Goff, Appl. Phys. Lett. **86**, 172503 (2005).
[15] R. Morel, A. Brenac, and C. Portemont, J. Appl. Phys. **95**, 3757 (2004).
[16] R. Morel, C. Portemont, A. Brenac, and L. Notin, Phys. Rev. Lett. **97**, 127203 (2006).
[17] V. Sessi, S. Hertenberger, J. Zhang, D. Schmitz, S. Gsell, M. Schreck, R. Morel, A. Brenac, J. Honolka, and K. Kern, J. Appl. Phys. **113**, 123903 (2013).
[18] E. Winkler, R. D. Zysler, H. E. Troiani, and D. Fiorani, Physica (Amsterdam) **384B**, 268 (2006).
[19] P. A. Kumar and K. Mandal, J. Appl. Phys. **101**, 113906 (2007).
[20] S. Stoyanov, V. Skumryev, Y. Zhang, Y. Huang, G. Hadjipanayis, and J. Nogués, J. Appl. Phys. **93**, 7592 (2003).
[21] D. Tobia, E. Winkler, R. D. Zysler, M. Granada, H. E. Troiani, and D. Fiorani, J. Appl. Phys. **106**, 103920 (2009).
[22] J. Sort, V. Langlais, S. Doppiu, B. Dieny, S. Suriñach, J. S. Muñoz, M. D. Baró, C. Laurent, and J. Nogués, Nanotechnology **15**, S211 (2004).
[23] X. F. Zhao, Y. C. Zhang, S. L. Xu, X. D. Lei, and F. Z. Zhang, J. Phys. Chem. C **116**, 5288 (2012).
[24] M. Artus, S. Ammar, L. Sicard, J. Y. Piquemal, F. Herbst, M. J. Vaulay, F. Fiévet, and V. Richard, Chem. Mater. **20**, 4861 (2008).
[25] S. P. Pati, B. Bhushan, A. Basumallick, S. Kumar, and D. Das, Mater. Sci. Eng. B **176**, 1015 (2011).
[26] B. Kuerbanjiang, U. Wiedwald, F. Haering, J. Biskupek, U. Kaiser, P. Ziemann, and U. Herr, Nanotechnology **24**, 455702 (2013).
[27] C. Portemont, R. Morel, A. Brenac, and L. Notin, J. Appl. Phys. **100**, 033907 (2006).

[28] Y. Yamamoto, H. Nakagawa, and H. Hori, J. Magn. Magn. Mater. **310**, 2384 (2007).
[29] L. Y. Lu, X. G. Xu, W. T. Zhang, J. Miao, and Y. Jiang, Mater. Lett. **64**, 2424 (2010).
[30] N. Banerjee, J. W. A. Robinson, and M. G. Blamire, Nat. Commun. **5**, 4771 (2014).
[31] P. K. Manna and S. M. Yusuf, Phys. Rep. **535**, 61 (2014).
[32] I. V. Golosovsky, G. Salazar-Alvarez, A. López-Ortega, M. González, J. Sort, M. Estrader, S. Suriñach, M. D. Baró, and J. Nogués, Phys. Rev. Lett. **102**, 247201 (2009).
[33] N. H. Hai, N. M. Dempsey, and D. Givord, Eur. Phys. J. B **24**, 15 (2001).
[34] See Supplemental Material at http://link.aps.org/supplemental/10.1103/PhysRevLett.115.057201 for experimental details, the mean-field model, and supplemental figures.
[35] J. A. De Toro, J. A. González, P. S. Normile, P. Muñiz, J. P. Andrés, R. López Antón, J. Canales-Vázquez, and J. M. Riveiro, Phys. Rev. B **85**, 054429 (2012).
[36] R. López Antón, J. A. González, J. P. Andrés, J. Canales-Vázquez, J. A. De Toro, and J. M. Riveiro, Nanotechnology **25**, 105702 (2014).
[37] M. Gracia-Pinilla, E. Martínez, G. S. Vidaurri, and E. Pérez-Tijerina, Nanoscale Res. Lett. **5**, 180 (2009).
[38] D. Schumacher, A. Steffen, J. Voigt, J. Schubert, Th. Brückel, H. Ambaye, and V. Lauter, Phys. Rev. B **88**, 144427 (2013).
[39] J. Nogués, V. Skumryev, J. Sort, S. Stoyanov, and D. Givord, Phys. Rev. Lett. **97**, 157203 (2006).
[40] G. Margaris, K. N. Trohidou, and J. Nogués, Adv. Mater. **24**, 4331 (2012).
[41] Note that although shifted loops with $H_C < H_E$ may not be useful for recording or other applications, centered loops with similar enhanced effective anisotropy can be obtained when cooling in ac fields; see N. J. Gökemeijer and C. L. Chien, J. Appl. Phys. **85**, 5516 (1999).
[42] A. Schrön, C. Rödl, and F. Bechstedt, Phys. Rev. B **86**, 115134 (2012).
[43] S. Soeya, M. Fuyama, S. Tadokoro, and T. Imagawa, J. Appl. Phys. **79**, 1604 (1996).
[44] J. McCord, R. Kaltofen, T. Gemming, R. Hühne, and L. Schultz, Phys. Rev. B **75**, 134418 (2007).
[45] A. C. Johnston-Peck, J. W. Wang, and J. B. Tracy, ACS Nano **3**, 1077 (2009).
[46] A. Roy, J. A. De Toro, V. S. Amaral, P. Muniz, J. M. Riveiro, and J. M. F. Ferreira, J. Appl. Phys. **115**, 073904 (2014).
[47] C. Ge, X. Wan, E. Pellegrin, Z. Hu, S. M. Valvidares, A. Barla, W. I. Liang, Y. H. Chu, W. Zou, and Y. Du, Nanoscale **5**, 10236 (2013).
[48] M. J. Carey, A. E. Berkowitz, J. A. Borchers, and R. W. Erwin, Phys. Rev. B **47**, 9952 (1993).
[49] M. J. Carey and A. E. Berkowitz, J. Appl. Phys. **73**, 6892 (1993).
[50] E. N. Abarra, K. Takano, F. Hellman, and A. E. Berkowitz, Phys. Rev. Lett. **77**, 3451 (1996).
[51] C. A. Ramos, D. Lederman, A. R. King, and V. Jaccarino, Phys. Rev. Lett. **65**, 2913 (1990).
[52] J. A. Borchers, M. J. Carey, R. W. Erwin, C. F. Majkrzak, and A. E. Berkowitz, Phys. Rev. Lett. **70**, 1878 (1993).
[53] K. Akmaldinov, C. Ducruet, C. Portemont, I. Joumard, I. L. Prejbeanu, B. Dieny, and V. Baltz, J. Appl. Phys. **115**, 17B718 (2014).
[54] It is worth mentioning that similar high-temperature stabilization could probably be obtained using pure high-T_N or high-K AFMs (PtMn, NiMn, or IrMn), though some of these AFMs may require high-temperature processing, which could be incompatible with nanoparticles.
[55] N. J. O. Silva, I. Puente-Orench, M. Martins, T. Trindade, A. Millán, J. Campo, and F. Palacio, J. Phys. Conf. Ser. **325**, 012020 (2011).
[56] G. Vallejo-Fernandez, L. E. Fernandez-Outon, and K. O'Grady, Appl. Phys. Lett. **91**, 212503 (2007).
[57] J. Nogués and I. K. Schuller, J. Magn. Magn. Mater. **192**, 203 (1999).
[58] P. S. Normile, J. A. De Toro, T. Muñoz, J. A. González, J. P. Andrés, P. Muñiz, R. E. Galindo, and J. M. Riveiro, Phys. Rev. B **76**, 104430 (2007).
[59] D. L. Peng, K. Sumiyama, T. Hihara, S. Yamamuro, and T. J. Konno, Phys. Rev. B **61**, 3103 (2000).
[60] W. Han, R. K. Kawakami, M. Gmitra, and J. Fabian, Nat. Nanotechnol. **9**, 794 (2014).
[61] W. Liu, L. He, Y. Xu, K. Murata, M. C. Onbasli, M. Lang, N. J. Maltby, S. Li, X. Wang, C. A. Ross, P. Bencok, G. van der Laan, R. Zhang, and K. L. Wang, Nano Lett. **15**, 764 (2015).
[62] C. La-o-vorakiat, Y. Tian, T. Wu, C. Panagopoulos, J. X. Zhu, H. Su, and E. E. M. Chia, Appl. Phys. Lett. **104**, 141602 (2014).
[63] S. Singh, J. T. Haraldsen, J. Xiong, E. M. Choi, P. Lu, D. Yi, X. D. Wen, J. Liu, H. Wang, Z. Bi, P. Yu, M. R. Fitzsimmons, J. L. MacManus-Driscoll, R. Ramesh, A. V. Balatsky, J. X. Zhu, and Q. X. Jia, Phys. Rev. Lett. **113**, 047204 (2014).
[64] S. H. Nie, Y. Y. Chin, W. Q. Liu, J. C. Tung, J. Lu, H. J. Lin, G. Y. Guo, K. K. Meng, L. Chen, L. J. Zhu, D. Pan, C. T. Chen, Y. B. Xu, W. S. Yan, and J. H. Zhao, Phys. Rev. Lett. **111**, 027203 (2013).